Bulletins of Research Institute of Marine Science and Technology
Korea Maritime University, Vol. 4, pp. 67 - 88, December 1995.

NUMERICAL SIMULATIONS OF A PIPE UNDER COLLISION WITH HYDROCODE DYNA3D

Lee Sang-Gab*

ABSTRACT

Offshore structures are exposed to higher probability of collision with ship or icebergs because of their limited mobility. In general, the consequence of the collision is reported to be relatively small and it is desirable to consider minor collisions in the design stage. It is important to have a comprehensive understanding of the dynamic responses of a pipe, their main member, under collision to design offshore strucrure against possible accidents.

It is needed to estimate the probable extent of damage of a pipe, depth of dent, affected by the time history of impact load in order to design a pipe strong enough for collision. In this paper, dynamic behaviors of a pipe due to the lateral impact are investigated through the numerical simulations with hydrocode DYNA3D, a three dimensional elasto-plastic large deformation impact contact problem analyzing program.

The dynamic responses to a pipe under collision are examined. The effect of strain rate sensitivity of the yield stress is examined. Rate sensitive damage model for describing the macroscale behavior of sea ice is also implemented to the material type in code DYNA3D for numerical simulation of iceberg indentation. The validity of code DYNA3D is confirmed by the published experimental results.

Key Words : offshore strucrure, pipe, collision, lateral impact, DYNA3D, extent of damage, macro ice mechanics, strain rate sensitivity.

INTRODUCTION

There has been a growth of interest in offshore collision problems with ship such as attendant vessel, loading tanker and passing vessel etc., whose consequencies have been reported to be relatively small[1-3]. A collision with an offshore structure can be classified into major and minor based on the extent of its damage. A minor collision will results in repairable local damage of the structure, while a major one

* Korea Maritime University, Dept. of Naval Architeature

will damage it globally. It seems extremely uneconomical to design it to withstand a major collision, and the probability of major collisions should be kept at a low level by means of adequate preventive measures.

It is desirable, therefore, to consider minor collisions in the design stage, and necessary to predict their probability and the probable extents of damage. Standing and Brending[1] provided probable ranges of the collision velocity for four scenarios: heave collision at the stern, collision when alongside, collision when maneuvring, and collision of drifting vessel. The distribution of collision velocity is found to be insensitive to vessel size, and the modern supply vessel tends toward increase of its size. It is still premature to predict the actual collision probability and the probable extents of damage.

By the assumptions commonly adopted in the static approach dynamic effects are insignificant and the elastic strain energy stored in the colliding bodies is negligible. According to the results of the recently published works these assumptions cannot be valid[4]. It would be premature to draw any firm conclusions from the results of the limited cases, but it can be suggested that dynamic elastic-plastic analyses must be employed in predicting the consequences of offshore collisions. More reliable simulation methods are necessary, owing to the complexity and the uncertainty in the nature of offshore collision.

Recently, according to be known that arctic regions have a lot of cruid oil, natural gas and resource deposits, artic engineering field takes a growing interest in many countries as a technical basis for the construction of arctic offshore structures. icebreakers and other equipments. Particurarly, researches about the interaction between sea ice and offshore structure are performed extensively[5]. The complexity of sea ice behavior is due mainly to the strong dependence on rate of loading, the simultaneous occurrence of ductile, strain-softening and brittle modes of the deformation, the pressure sensitivity leading to different strengths in compression and tension, the material anisotropy, the strong dependence of temperature and internal structure of ice (grain size, fabric, brine volume, salinity, porosity)[6]. Uncertainties in existing ice models come primarily from the incomplete modeling of the mechanical behavior of ice in various loading states.

The cost of offshore structure for production in the Artic is significantly influenced by ice loads. The major design problem is to obtain suitable resistance to the large local ice load for both service and ultimate conditions. Global ice loads

govern the overall structural geometry and dimensions as well as the foundation design, while local ice pressure are likely to dictate wall thickness and local framing, and may well govern structural cost. Watt[7] has shown that peak local pressures may be as high as three times the average pressure assumed for global load. Numerical models are necessary for computer simulation of ice-structure interaction processes, which are affected by the following research concerns: rate dependent material behavior, simultaneous occurence of rate dependence and fracture behavior, time-varying contact between ice and structure and between fractures ice features, and strain-softening of ice.

The above mentioned crash or impact problems have a dominant characteristic of large deformation for short time scales with dynamic material plasticity. Code DYNA3D[8] is a general-purpose, explicit finite element program used to analyze the nonlinear dynamic response of three-dimensional inelastic structures. In this study, code DYNA3D is used to numerically simulate the dynamic response of a pipe under collision of rigid body and ice sheet or iceberg. Lateral impact simulations will be validated with experimental results[9], which were conducted on small-scale tubes having simply supported roller conditions.

The aim of this study is to perform numerical simulations of the probable extent of damage of unstiffened pipe subjected to lateral impact with code DYNA3D, and to establish a comprehensive understanding of the dynamic responses to a pipe under collision for next performing systematic parametric studies to design offshore strucrure. Strain-rate sensitivity of the material and other dynamic effects upon the response of a pipe under lateral impact have been considered. Rate sensitive damage model for describing the macroscale behavior of sea ice is implemented to the material type in code DYNA3D for numerical simulation of iceberg indentation.

VALIDATION OF CODE DYNA3D FOR NUMERIACL SIMULATIONS

To validate code DYNA3D to use in this study, it is desirable to compare the results of numerical simulations of code DYNA3D with experimental ones. Twenty four lateral impact tests were conducted on small scale tubulars having simply supported roller conditions by Cho[9]. The experimental tests were arranged with test rig and runway. A vertical aluminum wedge is attached on the front of the box of

the striker, whose angle is 45° and tip is sharp. The speed of the striker can be controlled by the heights of striker on the inclined runway. Simply supported roller conditions are adopted at both ends of test specimens, allowing free rotation and axial movement of the ends but no lateral movement. These can be availabe by the double hinged holders whose width is 50 mm. Two test results, models A3 and H2, are used in this study, whose measured model geometries, material properties and test results are as follows.

TABLE 2.1 Measured Model Geometries, Material Properties and Test Results [9]

Model	Length (mm)		Outer Diameter (mm)	Thickness (mm)	Static Yield Stress (MPa)	Young's Modulus (GPa)	Mass of Striker (kg)	Initial Velocity of Striker (m/s)	Depth of Dent (mm)
	Actual	Impact							
A3	1400	1350	50.88	1.23	472	200	18.8	2.34	3.5
H2	1400	1350	50.92	2.02	421	212	41.1	2.55	3.2

A quarter of numerical specimen is modeled using symmetric condition, and a half of model is shown in FIGURE 2(a). Striker consists of the wedge and hexadron parts and the density of hexadron controls the mass of striker. Striker is imposed to impact the midsection of a pipe along the length toward y axis direction, and the origin of x-y plane is located at the center of midsection. 8 node solid element in DYNA3D is used for a pipe and striker models. The ends of tubular are restrained as simply supported roller conditions similar to the experiments, allowing free rotation and axial movement of the end with width 25mm but no lateral movement.

Two kinds of material types are employed for numerical specimen: Isotropic Plasticity and Strain Rate Dependent Isotropic Plasticity. The former material type is used for striker. The same dimensions and material properties of each model in experimental test are used for numerical simulation. The density and Poisson's ratio of pipe and striker wedge to use here are 7850 kg/m^3 and 0.3, respectively.

Dented configurations of Model A3 are shown in FIGURE 2: Half of and whole configuarations at the maximum dentation are shown in FIGURE 2(b) and (c), repectively. FIGURE 2(d) shows the whole configuration after rebound of striker. The time history of effective stress of Model A3 and H2 at a point of impact is shown in FIGURE 3. The highest stresses occur at a point of impact and the near points along the midsection contour, and the maximum effective stresses are 115 MPa(Model A3) and 149 MPa(Model H2) which are very low compared to the static tensile yielding

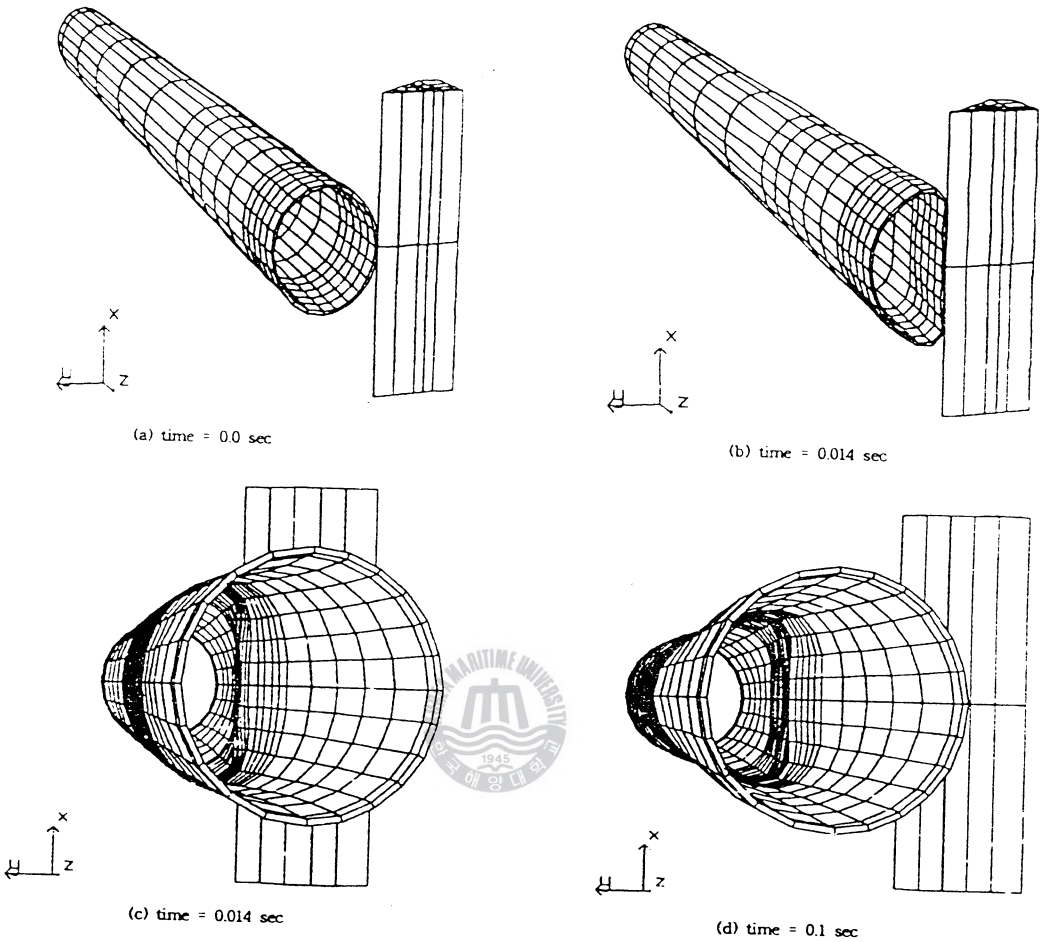

FIGURE 2.1 Numerical meshing and deformed geometry of Model A3

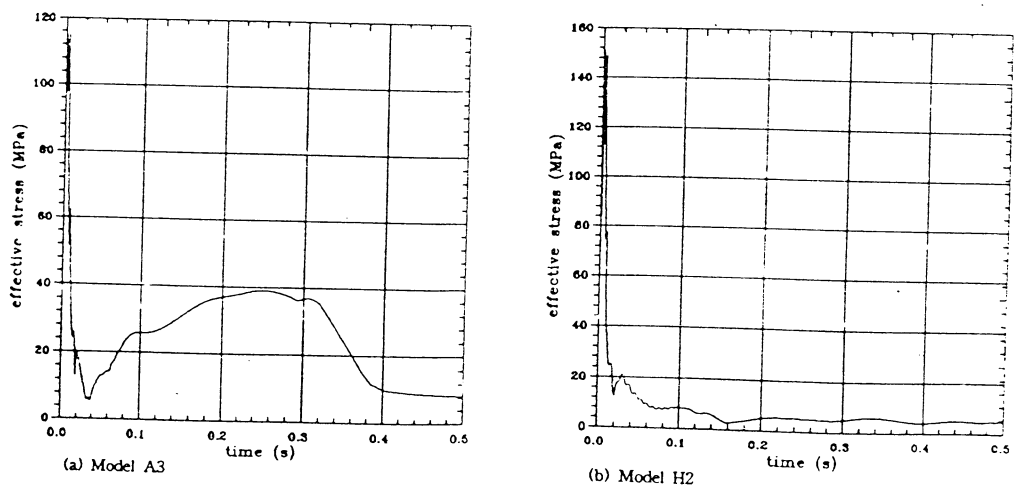

FIGURE 2.2 Time history of effective stress at a point of impact of pipe

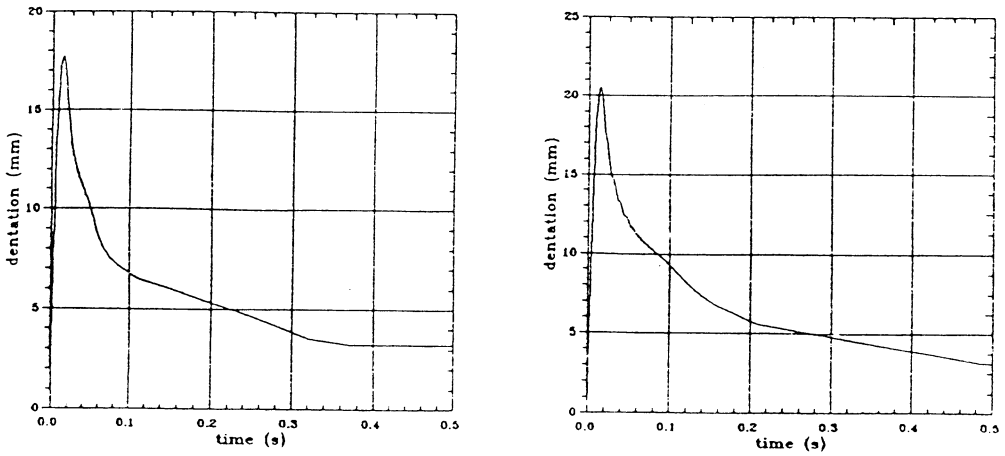

FIGURE 2.3 Time history of depth of dent of Model A3 and H2

stresses 472 and 421 MPa, repectively. It can be seen that the whole pipe still remains elastic state during impact with a low kinetic energy in this experiment. Therefore, the effect of strain rate will be discussed at the following section with a high kinetic energy.

The time history of depth of dent in the midsction of Model A3 and H2 can be seen in FIGURE 4 and the depths of dent at the end of impact are 3.25 mm(Moeld A3) and 3.12 mm(Model H2). Compared to the experimental results 3.5 mm(Model A3) and 3.2 mm(Model H2) in TABLE 2.1, it can be say that the numerical simulation results are very satisfactory. Even though the above numerical simulations are few to validate, it may say that the already acknowledged tool DYNA3D is sufficient to perform the impact problems.

NUMERIACL SIMULATIONS OF COLLISION WITH RIGID BODY

Numerical simulations of a pipe with impact of ship is performed to examine the dynamic effect. Geometries and boundary conditions of a pipe specimen are similar to the previous ones, and striker ship is idealized to the bulbous bow and hexahedron. Bulbous bow is modeled as a halh of sphere again. Pipe has the following dimensions; 1.5 m outer diameter, 3 cm thickness, 20 m length. Diameter of sphere is 1.0 m and hexahedron is mounted to the sphere whose density adjusts the striker

mass.. Young's modulus, Poisson's ratio and density of pipe and striker sphere for numerical simulation are 210 GPa, 0.3 and 7850 kg/m^3.

The relative mass of sruck and striker is important factor in the collision problem. In this study the mass and velocity of striker are only varied, while the ones of struck pipe are assumed to be fixed except one, yield stress. Sphere is assumed to be rigid and to impact at the midsection of a pipe along the length. The consideration of relative mass and deformable striker sphere will be tried in the following study. A quater of numerical specimen is also modeled using symmetric condition, and a half of model is shown in FIGURE 3.1(a).

Material type of strain rate dependent plasticity is employed for examing the material dynamic effect. A relationship for the calculation of dynamic yield stress proposed by Cowper and Symonds[10] is implemented to the material type of DYNA3D. It relates the dynamic yield stress σ_Y in the case of a uniaxial stress

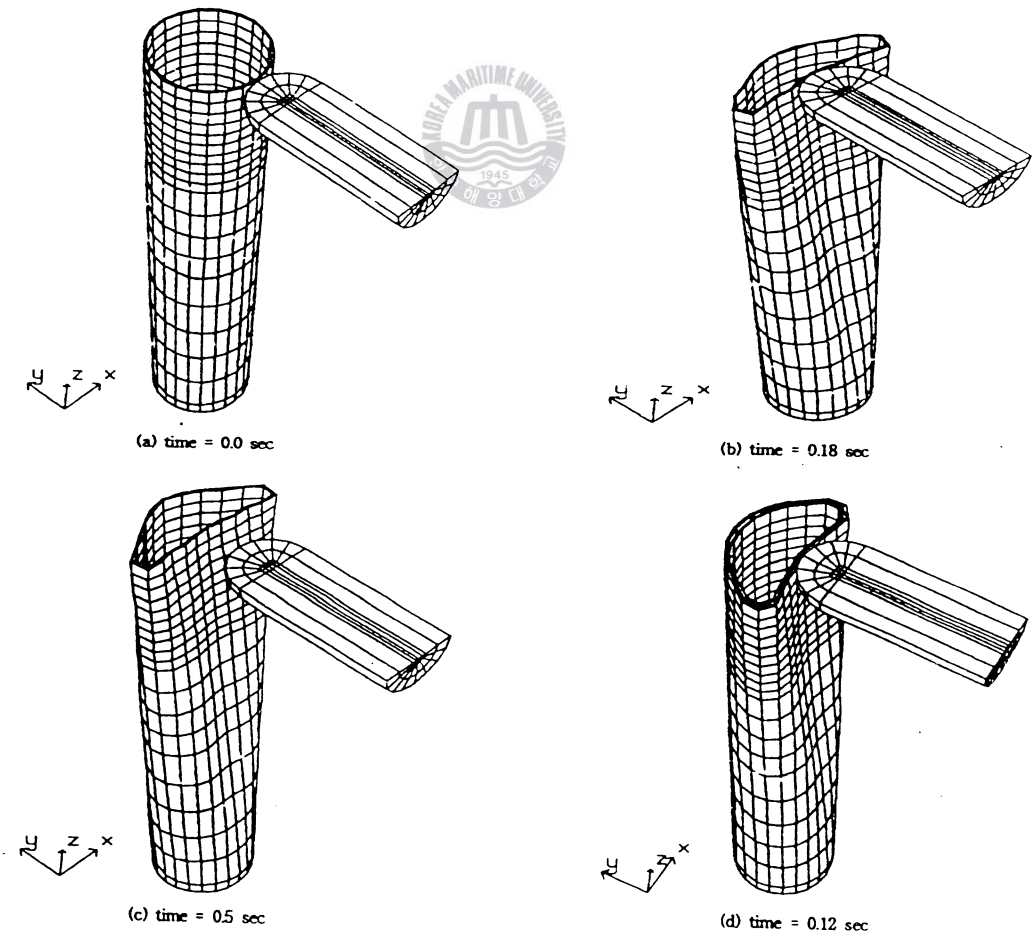

FIGURE 3.1 Numerical meshing and deformed geometry

system with stain rate $\dot{e}$ through the following expression

$$\frac{\sigma_Y}{\sigma_o} = 1 + (\frac{\dot{e}}{D})^{1/p} \tag{3.1}$$

where σ_o is the static yield stress, and D and p are constants. For mild steel, D equals 40.4 s^{-1} and p is equal to 5. In the case of a multiaxial stress system the uniaxial stress and strain values are replaced by equivalent stresses and strains.

The static inelastic material behavior, relationship of equivalent stress and equivalent plastic strain, is modeled as the following nonlinear isotropic hardening law with an exponential(saturation) part

$$\sigma(\bar{e}^p) = \sigma_o + (\sigma_u - \sigma_o)(1 - e^{-\gamma \bar{e}}) \tag{3.2}$$

where σ_u is the static ultimate stress, and γ is the initial rate of exponential hardening. The parameter $\bar{e}$ is a shifted equivalent plastic strain, allowing the modeling of a yield plateau, given by the expression

$$\bar{e} = \begin{cases} 0 & 0 \le \bar{e}^p \le \bar{e}_{sh} \\ \bar{e}^p - \bar{e}_{sh} & \bar{e}_{sh} \le \bar{e}^p \end{cases} \tag{3.3}$$

where $\bar{e}_{sh}$ is the length of the plastic plateau.

To examine the effect of material properties of pipe specimen to impact problem two types of material constants are used: Type 1(σ_o=250 MPa, σ_u=400 MPa), Type 2 (σ_o=415 MPa, σ_u=610 MPa). $\bar{e}_{sh}$=0.02 and $\bar{e}_u$=0.5 for both Type1 and Type 2, where $\bar{e}_u$ is the plastic strain at failure. The distribution of collision velocity and mass of striker is relatively various in the records of collisions[1], the usual cases are categorized into the mass under 2500 ~ 5000 ton and the velocity between 0.5 ~ 2.0 m/s. In this study collision prblem with 2000 ton striker at 0.5 m/s or 1.0 m/s velocity is basically considered to the above dimension pipe. To examine the dynamic effects of impact problems its velocity is increased instead of decreasing its mass keeping the same intial kinetic energy. Four Scenarios are considered, as shown in TABLE 3.1

TABLE 3.1 Description of 4 scenarios

	Velocity(m/s)	Mass(ton)	Initial Kinetic Energy (MN-m)	Material Type
Scenario 1	5.0	20	0.25	Type 1
	10.0	5		
Scenario 2	5.0	20	0.25	Type 2
	10.0	5		
Scenario 3	5.0	20	0.25	Type 2
	7.5	20	0.5625	
	10.0	20	1.0	
Scenario 4	10	20	1.0	Type 2
	20	5		
	30	2.222		

Scenarios 1 and 2 have the same initial kinetic energy 0.25 MN-m(0.5 m/s, 2000 ton), but the different yield and ultimate stresses, which will give an effect of material property. Scenario 3 is intented to examine the effect of velocity of striker with ths same mass varying kinetic energy from 0.25 ~ 1.0 MN-m. Scenario 4 will show the effects of relationship between velocity and mass of striker. with relative big initial kinetic energy 1.0 MN-m(1.0 m/s, 2000 ton). A half of the deformed configurations at the maximum dent and after rebound of typical case, 10 m/s and 20 ton, among the scenarios are shown in FIGURES 3.1(b) and (c). Time history of effective stress at the point of impact of piper, time history of depth of dent at the midsection of pipe, time history of velocity of striker and time history of kinetic energy of striker for each Scenario are presented at FIGURES 3.2-3.5, respectively. These results are summarized in TABLE 3.2.

It can be seen from FIGURE 3.2 and TABLE 3.2 that the peak of effective stress at the point of impact is increased a little with an increase of velocity of striker at the same lower initial kinetic energy in Scenario 1 and 2, and also increased somewhat with increasing velocity at the same mass of striker in Scenario 3. The same phenomenon can be found in Scenaio 4, but very big peak value occurs at high velocity, for example, over 20 m/s of velocity in this study. This symptom can be referred to the effect of strain rate dependent plasticity of material. The effect of strain rate will be discussed at the end of this section. Even the same condition is applied to the Scenarios 1 and 2, it can be seen that the peak of effective stress highly depends on the strength of material from FIGURES 3.2(a) and (b). From these results we may say that the stress of struck material greatly depends on the high speed of striker and the strength of struck material. The case of 5 m/s and 80 ton in

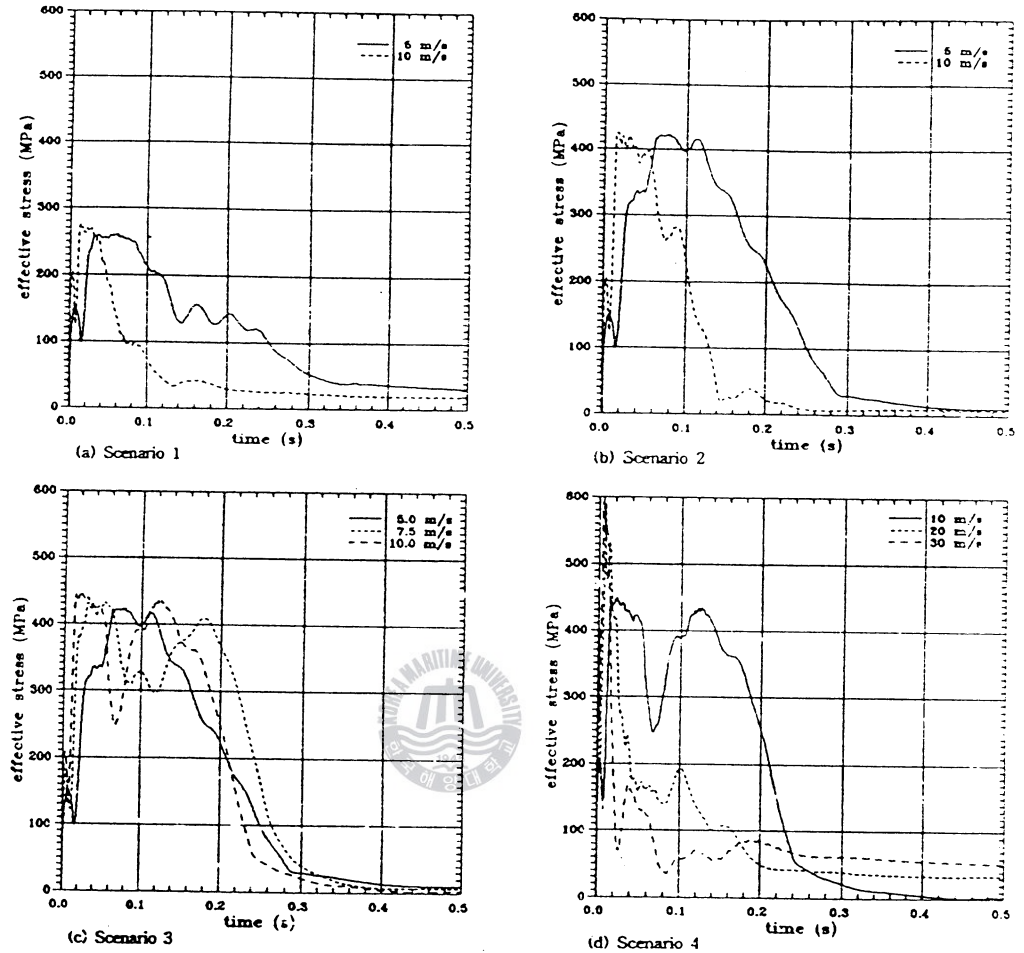

FIGURE 3.2 Time history of effective stress at a point of impact of pipe

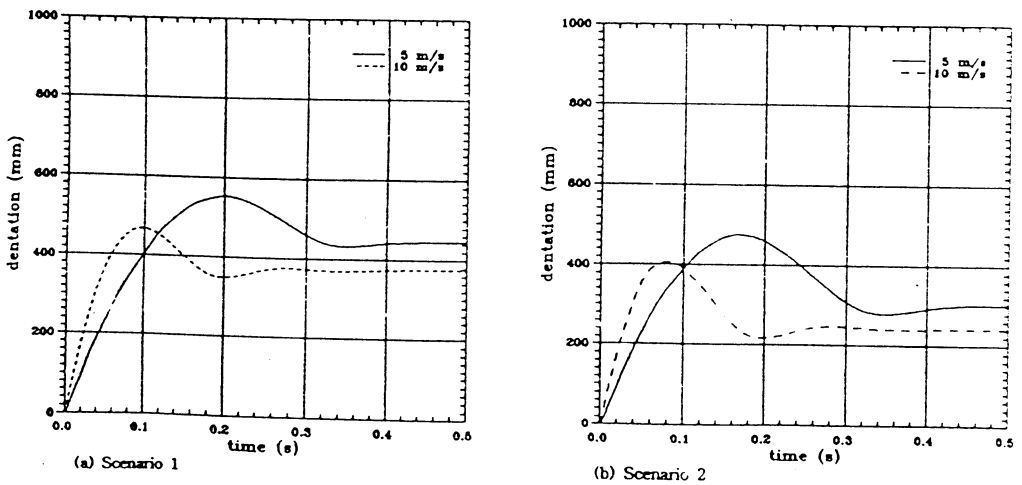

FIGURE 3.3 Time history of depth of dent at a midsection of pipe (continue)

Scenario 4, not shown in Figure, shows that the peak effective stress is much lower than the case of 30 m/s and 2.22 ton with even 36 times as big in mass.

TABLE 3.2 Results of numerical simulation for each Scenario

		Effective Stress(MPa)		Depth of Dent(mm)		Velocity(m/s)		Kinetic Energy ×1/4 (MN-m)	
		Max	Min	Max	Min	Max	Min	Max	Min
Scenario 1	5 m/s 20 t	261	31.0	554	446	5.0	-1.02	0.0625	0.0026
	10 m/s 5 t	276	24.6	469	377	10.0	-1.50	0.0625	0.0014
Scenario 2	5 m/s 20 t	422	10.3	476	306	5.0	-1.50	0.0625	0.0056
	10 m/s 5 t	425	7.0	406	242	10.0	-2.22	0.0625	0.0031
Scenario 3	5.0 m/s 20 t	422	10.3	476	306	5.0	-1.50	0.0625	0.0056
	7.5 m/s 20 t	430	6.8	713	526	7.5	-1.70	0.1406	0.0072
	10.0 m/s 20 t	449	3.2	975	794	10.0	-1.93	0.2500	0.0092
Scenario 4	5.0 m/s 80 t	438	18.7	1120	959	5.0	-0.98	0.2500	0.0095
	10.0 m/s 20 t	449	3.2	975	794	10.0	-1.93	0.2500	0.0092
	20.0 m/s 5 t	590	33.3	819	627	20.0	-2.55	0.2500	0.0040
	30.0 m/s 2.2 t	599	52.4	702	521	30.0	-2.96	0.2500	0.0024

On the contrary to the case of the effective stress, the depth of dent at the midsection of pipe can be seen to be greatly dependent on the mass of striker at the same kinetic energy, and on the speed of striker at the same mass of striker, as shown in FIGURE 3.3 and TABLE 3.2. Compared to Scenario 1 and 2, high strength of material can sustain more the deformation from the impact than low strength of material. Therefore, deformation by impact is more affected by the increase of mass at the same kinetic energy, and largely by the speed of striker at the same mass of striker, and finally by the strength of material. The residual deformation also has the same phenomenon.

As expected, rebounding velocity of striker is increased a little with an increase of initial impact velocity of striker, as shown in FIGURE 3.4 and TABLE 3.2. Rebounding velocity is also increased a bit with decreasing mass of striker at the same initial velocity. Striker is rebounded more quickly as initial velocity is increased at the same initial kinematic energy, while striker is rebounded at the same time in the case of the same mass of striker. The high strength of struck material rebounds a striker somewhat faster than the low strength.

Initial kinetic energy of striker, $E = 1/2\ MV^2$, can be determined by the mass, impact velocity, impact geometries, etc.. Since rebounding velocity of striker is not proportional to the initial impact one, kinetic energy after rebound can be found to be

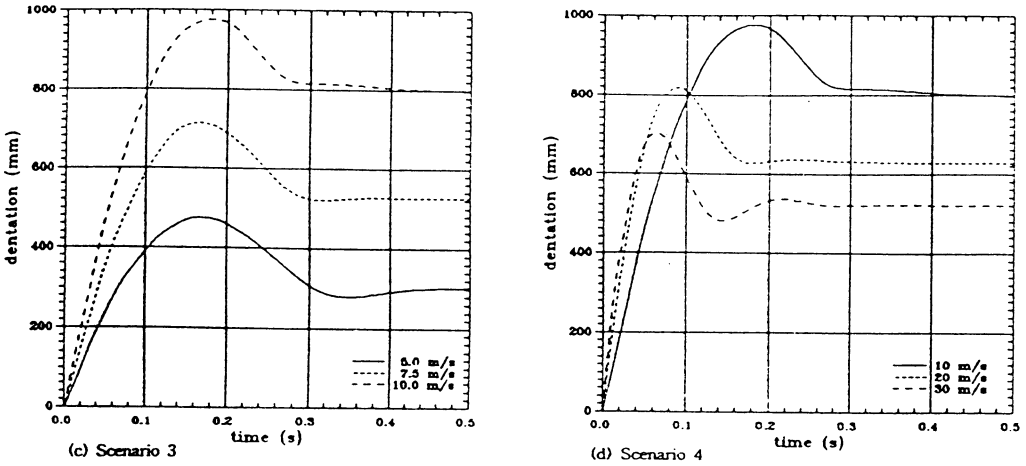

FIGURE 3.3 Time history of depth of dent at a midsection of pipe

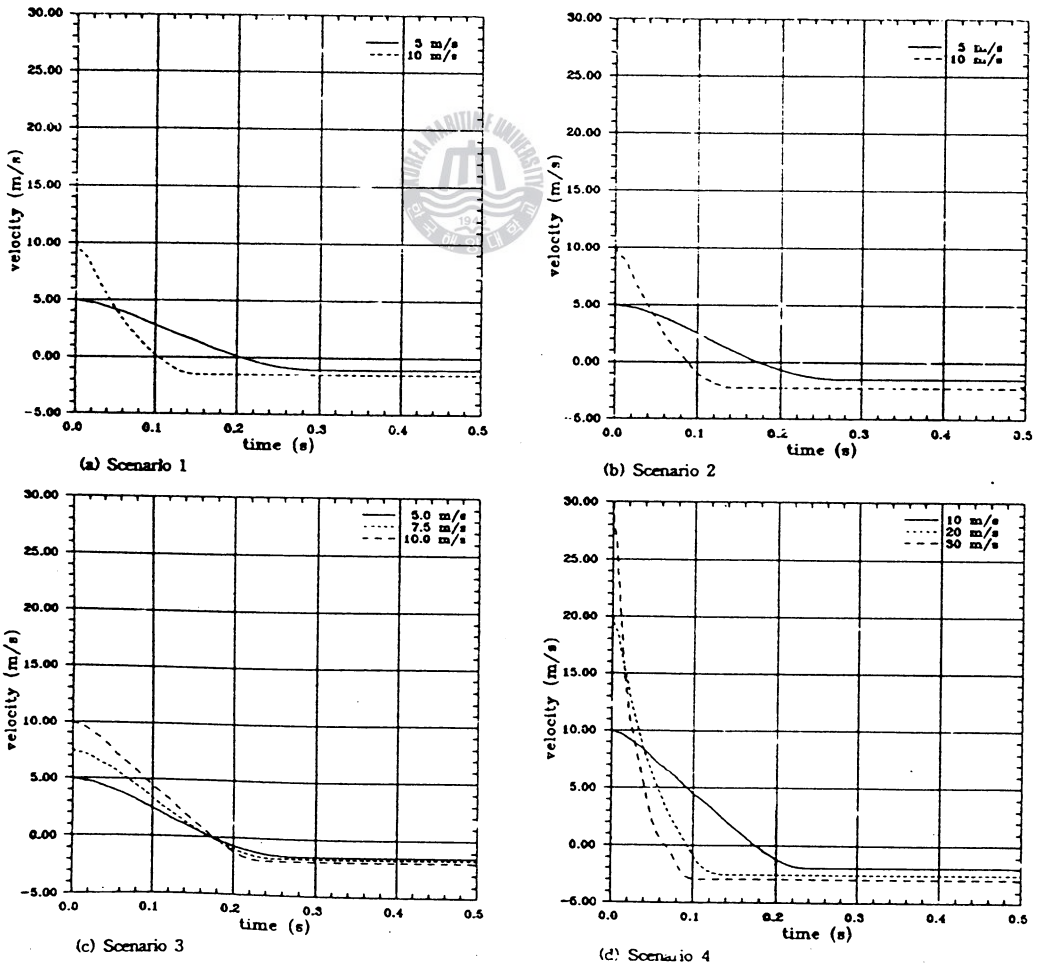

FIGURE 3.4 Time history of velocity of struck pipe

affected more by the mass of striker at the same kinetic energy, as shown in FIGURE 3.5 and TABLE 3.3. Kinetic energy after rebound must be be affected more by the speed of striker at the same mass. Since striker is relatively rigid, there is no deformation of striker during impact. Therefore, it may be said that the total absorbed energy of pipe and kinetic energy of striker are the same, and no increase occurs from the impact. It can expected that the absorbed energy of struck body will be increased by the impact of deformable striker, which will be studied in the following study.

To examine the effect of strain rate of struck material, the dynamic yield stress implemented in DYNA3D in this study is not considered in the case of 20 m/s and 5 ton in Scenario 4. In this case, two types of static inelastic material behavior is set: Type 1 (existence of yield plateau $\bar{e}_{sh}$=0.02) and Type 2 (no existence of yield plateau $\bar{e}_{sh}$=0.00). Their results are shown in FIGURE 3.6. It can be seen that the peak effective stresses are 415 MPa in Type 1 and 442 MPa in Type 2, and the depths of dent are decreased by 26 mm in Type 1 and 19 mm in Type 2. Therefore increase of stresses around area near to the point of impact by the effect of strain rate gives somewhat resistance to deformation from the impact. Since the effective plastic strain is 0.01389 at the peak stress in Type 1, static inelastic stress must be 415 MPa and is on the yield plateau. It can be obtained that its strain rate is approximately 0.54 s^{-1} using Eq. 3.1.

Pile is usually inserted in the leg of offshore structure to fix the whole structure against the foundation. To examine the effect of pile in the leg on the impact, the following pile is considered inside a pipe: outer diameter 1.38 m, thickness 30 mm and space 30 mm between pile and pipe. The case of 10 m/s and 20 ton in Scenario 4 is performed, and its effect and the deformed configuration at maximum dent are shown in TABLE 3.3 and FIGURE 3.1(d), repectively. It can be seen that pile has a great effect on the resistance to the impact.

TABLE 3.3 Effcet of pile on the impact in the case 10 m/s and 20 ton

	Effective Stress(MPa)		Depth of Dent(mm)		Velocity(m/s)		Kinetic Energy ×1/4 (MN-m)	
	Max	Min	Max	Min	Max	Min	Max	Min
without pile	449	3.2	975	794	10.0	-1.93	0.2500	0.0092
with pile	465	4.7	648	467	10.0	-2.11	0.2500	0.0111

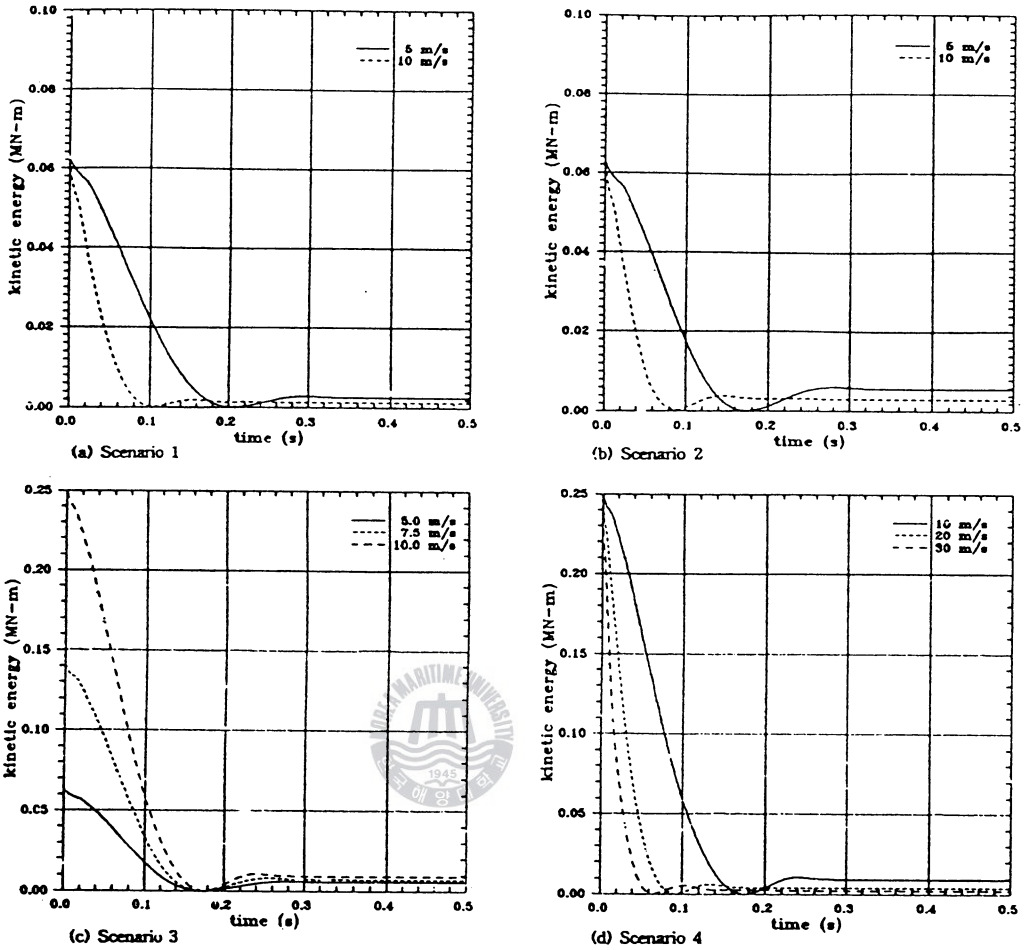

FIGURE 3.5 Time history of kinetic energy of striker

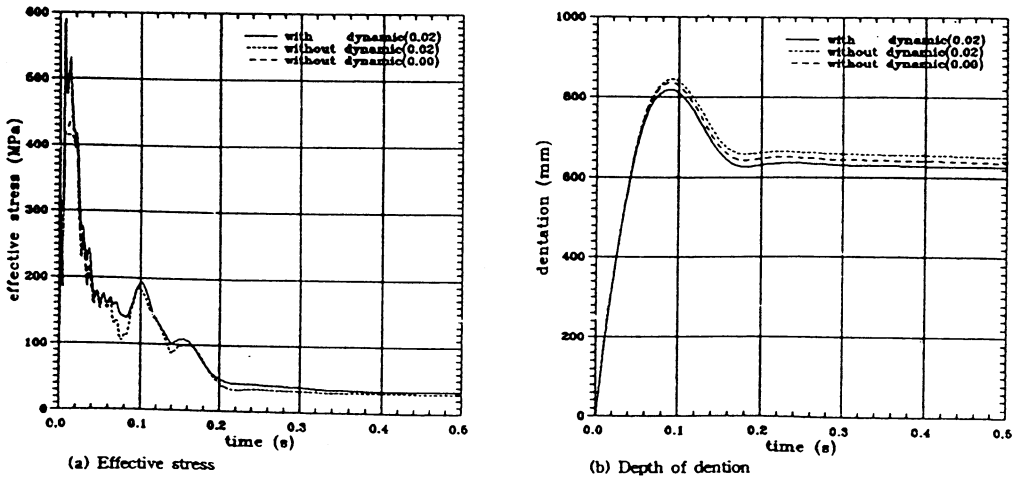

FIGURE 3.6 Effect of strain rate-dependent plasticity

NUMERIACL SIMULATIONS OF COLLISION WITH ICEBERG

Sea ice is an important feature in the Arctic, and the major difference between sea ice and fresh water ice is the amount of salts. Concerning the strength of ice, it is necessary to distinguish two different meanings, i.e. the fracture strength and the yield strength, which correspond to completely different failure modes. The brittle behavior of polycrystalline ice is characterized by elastic deformation followed by a sudden fracture, while ice in ductile condition may fail by yielding instead of fracture and this yield strength corresponds to the maximum stress that the ice can resist during deformation.

The deformation behavior, failure mechanism, and strength of ice are highly influenced by the strain rate. Ranges of strain rate may be classified as ductile, transitional and brittle. Laboratory model indentation tests were conducted and the strain rate was estimated as the indentational rate $U/\alpha B$, which is the strain rate of the indentor front. U is the interaction speed and B, the indentor width. Two results from uniaxial compressive test and indentation one are reported to be the same at $\alpha = 4$, as shown in FIGURE 4.1[11]. The above data rearranged as the following Eq. 4.1 is used for the numerial ice model in this study[5], where σ_{cf} is the compressive failure stress, $\dot{e}$ is equivalent indentational rate and the transition strain rate is set to $10^{-3.55}$ here.

$$\sigma_{cf} = \begin{cases} 10^{4.96} \times (\dot{e})^{0.31406} \text{ kPa} & (\dot{e} < 10^{-3.55}) \\ 7,000 \text{ kPa} & (10^{-3.55} \le \dot{e} < 10^{-2.65}) \\ 7,720 - 322,100 \times \dot{e} \text{ kPa} & (10^{-2.65} \le \dot{e} < 10^{-2.0}) \\ 4,500 \text{ kPa} & (10^{-2.0} \le \dot{e}) \end{cases} \quad (4.1)$$

The failure strain date occurs at approximately 1% strain for constant strain rate tests and there is a corresponding relation for constant stress tests, too. Failure strains are decreased with increasing strain rate above the transition strain rate[12]. The failure strain is assumed to have a constant value 1% through the strain rate for simplification. The above ice models are implemented to the material type in DYNA3D. It is assumed that the yield stress and failure stress are coincident through the strain rate. The other material properties of ice used here is as follows: Young's modulus 6.0 GPa, Poisson's ratio 0.3 and density 910 kg/m^3.

Steel member of offshore structure in Artic has to be designed considering the

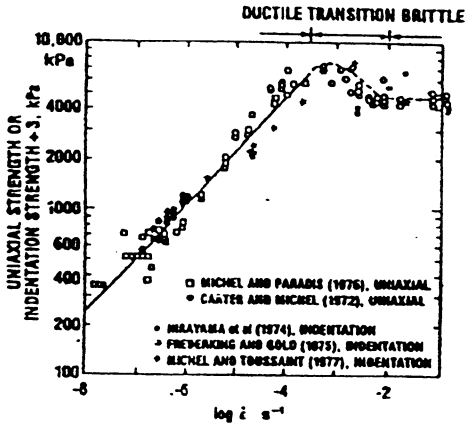

FIGURE 4.1 Proposed universal curve for indentation test data[11]

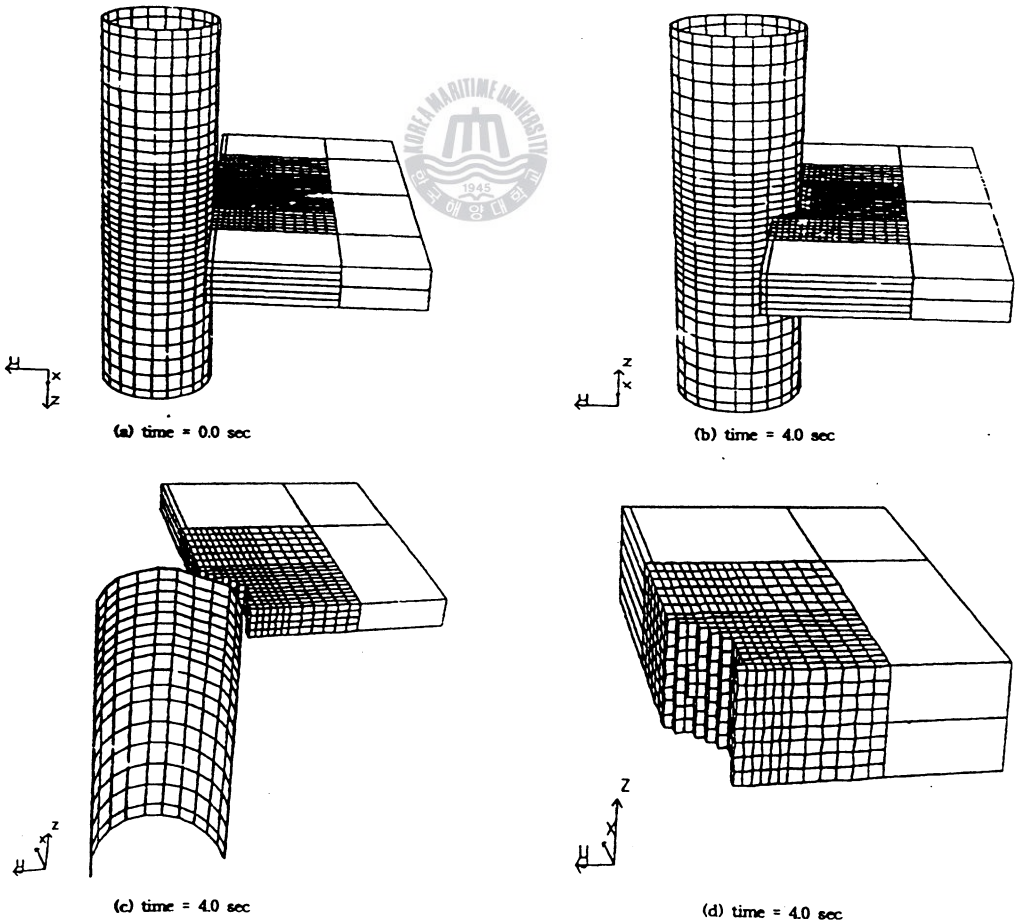

FIGURE 4.2 Numerical meshing and deformed geometry

regulations of AISC, API RP 2A-WSD, Dn V. Structural steel has to be followed the regulation of material properties in section 8 of API RP 2A-WSD, for example, Class A and Class B are allowed under low temperature. Study is needed more for the material properties of structureal steel member in Artic. In this study, however, attention is to be focused to the modeling of sea ice. Most of material properties of pipe are the same as the previous one: static yield stress 415 MPa and static ultimate stress 610 MPa(Class A). Material type of strain rate dependent plasticity is also employed for the material of pipe member.

Since braces of offshore structure in Artic are desirable to be located below the water to avoid the collision from ice sheet or iceberg, diameter of the multi-leg of Jacket type structure is usually large[5]. In this study unstiffened pipe member of leg is assumed to have the following dimensions: 6 m outer diameter, 50 mm thickness and 20 m length. Iceberg of 2 m depth is set to collide the midsection of pipe member. Two scenarios are performed with the same initial kinetic energy of striker iceberg for the numerical simulations of coillision with iceberg: Scenario 1(1 m/s, 4000 ton) and Scenario 2(2 m/s, 1000 ton). The whole model of the numerical simulations is shown in FIGURE 4.2(a). Boundary conditions at both ends of pipe are the same as the previous one: simply supported roller conditions, allowing free rotation and axial movement of the ends but no lateral movement.

A quarter of numerical specimen is also used by the symmetric condition. The radius of pipe specimen in a quarter modeling is 3.0 m, and it is reasonable to mesh an ice model at area 6.0 m × 6.0 m in x-y plane at the low impact velocity, as shown in FIGURE 4.2(a). Rigid bodies are attached to the back and at the side of the ice model, and control the ice total mass. FIGURE 4.2(b) shows the whole deformed configuration of a dented pipe and a partially crushed ice departing after impact. FIGURE 4.2(c) shows a quater of its configuration, and FIGURE 4.2(d), the half of its ice.

It can be seen from FIGURE 4.3 that the maximum peak of effective stress at the point of impact of pipe in Scenario 2 is a little higher (aproximate 25 MPa) and its interval is shorter (aproximate 0.16 sec) than in Scenario 1. Contrary to the impact problem with rigid body, the maximum magnitude of depth of dent at the midsection of pipe are almost the same with different velocity of striker at the same initial kinetic energy both in Scenarios 1 and 2, as shown in FIGURE 4.4. It can be also found from FIGURES 4.3 and 4.4 that peak points of effective stress and depth of

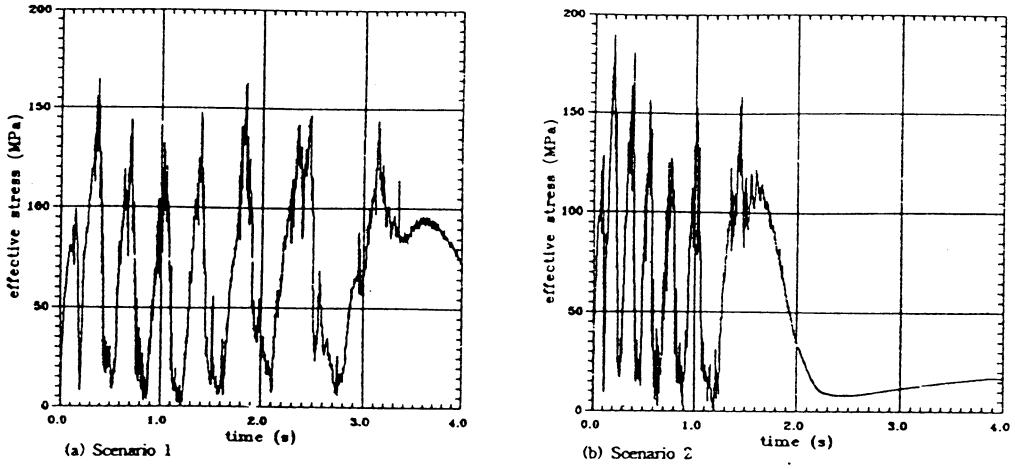

FIGURE 4.3 Time history of effective stress at a point of impact of pipe

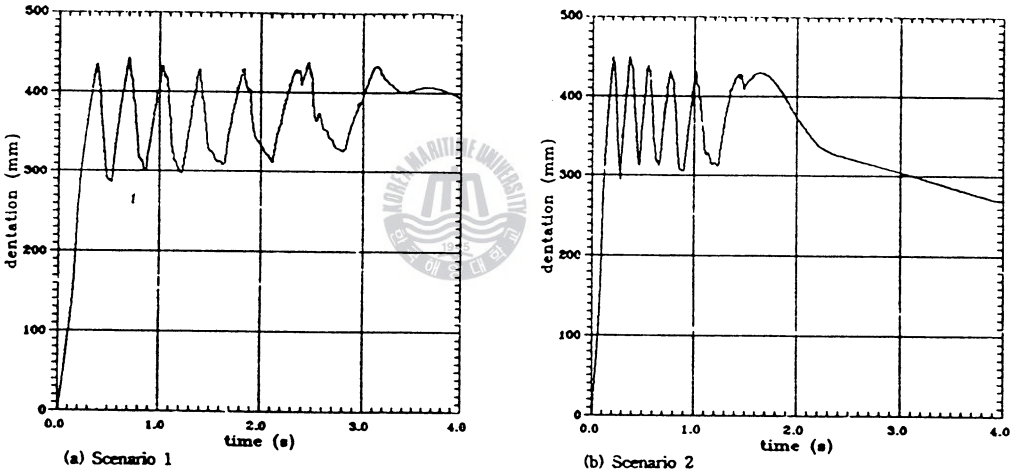

FIGURE 4.4 Time history of depth of dent at a midsection of pipe

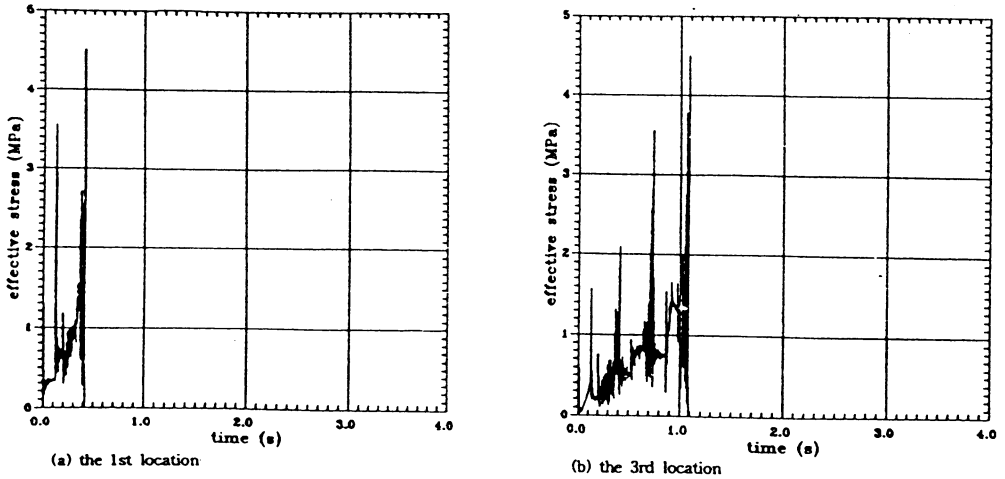

FIGURE 4.5 Time history of effective stress of ices at center (continue)

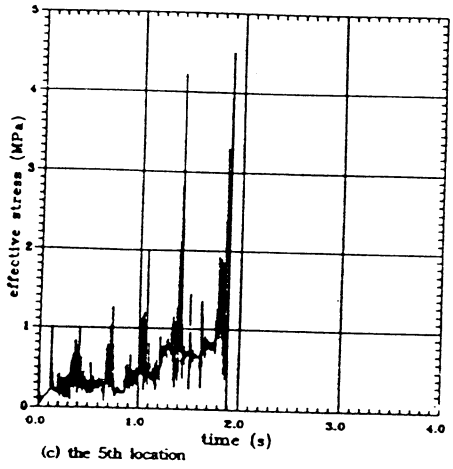

(c) the 5th location

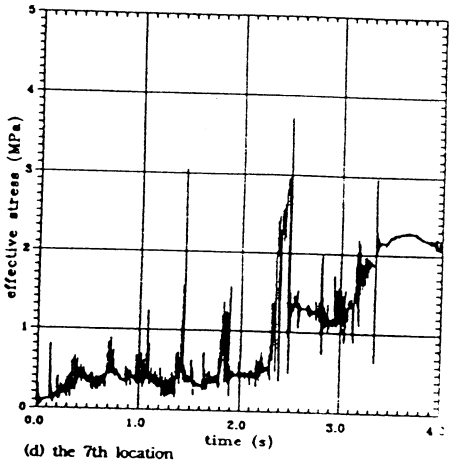

(d) the 7th location

FIGURE 4.5 Time history of effective stress of ices at center

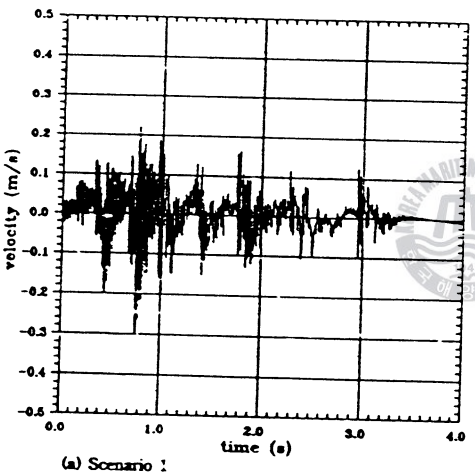

(a) Scenario 1

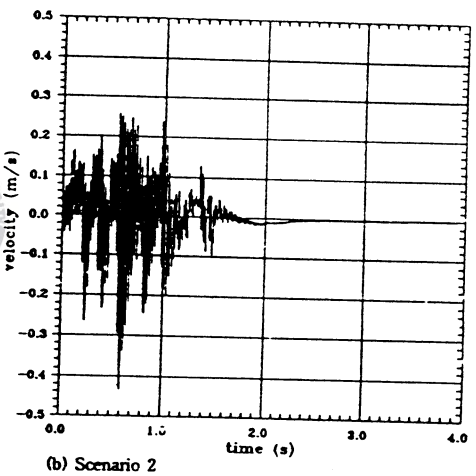

(b) Scenario 2

FIGURE 4.6 Time history of velocity at a point of impact of pipe

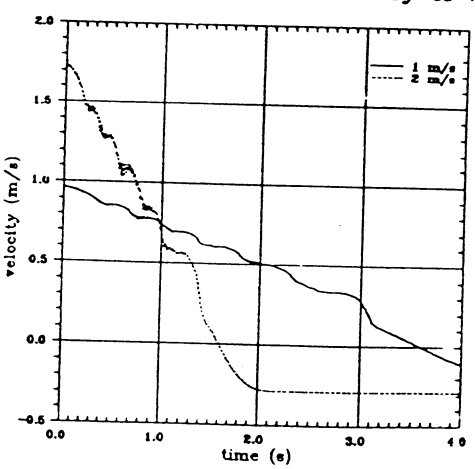

(a) Scenario 1

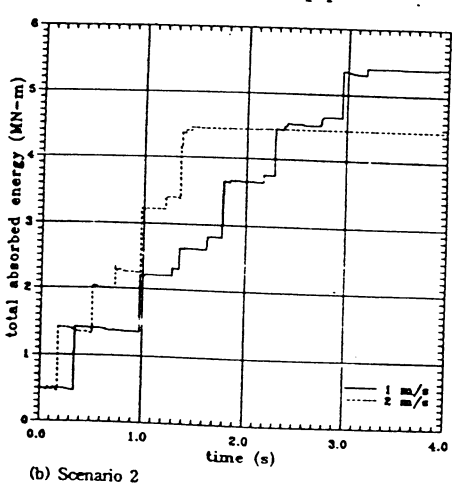

(b) Scenario 2

FIGURE 4.7 Time history of ice velocity FIGURE 4.8 Total absorbed energy of pipe

dent coincidently occurs in each Scenario. It can be recognized from FIGURE 4.5 that these phenomena come from the fracture of striker ice. FIGURE 4.5 shows a serial failure stresses of every two ice element at its fracture state from the first element to the seventh one in ice from the point of impact along the center line in Scenario 1: the 1st ice element(0.415 sec, 4.51 MPa), the 3rd one(1.08 sec, 4.51 MPa), the 5th one(1.89 sec, 4.51 MPa) and the 7th one(no fracture). Fracture stress 4.51 MPa occurs at failure effective strain 0.01, and strain rate during this time is approximately $10^{-4.15785}$ which can be obtained from Eq. 4.1. It can be guessed that ice behavior is in the ductile mode of the deformation and is close to the strain-softening stage.

Time histories of the velocities of pipe and iceberg in Scenario 1 and 2 are shown in FIGURES 4.6 and 4.7, repectively. As can be expected, iceberg with 2.0 m/s velocity and 1000 ton mass rebounds earlier at larger rebounding velocity than one with 1.0 m/s velocity and 4000 ton mass. It can be seen that pipe member impacted by the former iceberg globally vibrates larger and shorter than the one by the latter one. Contrary to the impact by the rigid body as the previous section, total absorbed energy of struck pipe is increased during contact with striker iceberg, as shown in FIGURE 4.8. Local load is elastically increased during contact of ice and pipe, ice is crushed when the load reaches to the fracture strength of ice, and a new ice again contacs pipe. As this process is repeated, pipe absorbs strain energy from the iceberg. This story can be found here by the numerical simulations of iceberg impact problems. Impact by the heavy mass with low velocity gives rather big absorbed strain energy than the one by the light mass with high velocity at the same kinetic energy. It can be recognized that the above results are affected by the size of ice element, which was 300 mm × 300 mm × 250 mm. It is expected that more small size of ice element will give a more smooth response.

CONCLUSIONS

In this paper, dynamic behaviors of a pipe under collision are investigated through the numerical simulations with hydrocode DYNA3D. This numerical simulation with code DYNA3D can be a powerful tool to establish a comprehensive understanding of the dynamic behavior of collisions problem and to estimate the probable extent of damage with accuracy, through the validity of this code by

comparing with the published experimental results.

During use of this code to the impact problems the followings are felt: Even this code plays a good numerical simulator to collision problems, many efforts are needed to use, especially in the implementaion of an exact material modeling. More basic informations to the impact problems are also needed for the good results of design step.

More basic numerical simulations for the relationship of striker mass and struck mass, and the effect of deformable striker etc., will be performed to the future study. Based on these basic informations, systemaic parametric studies will be considered for the design of offshore structure under collision: The effects of size and thickness of a pipe, type and size of its stiffener and boundary conditions are examined with respect to the mass and the initial velocity.

REFERENCE

[1] Standing, R.G. and Brending, W., "Collision of Attendant Vessels with Offshore Installations: Part 1 - General Description and Principal Results", Dept. of Energy(UK) Offshore Technology Report OTH84208, HMSO, London, 1985.

[2] Nataraja, R. and Pemsing, K., "Impact Energy due to Supply Vessel Collision: Case Studies", Proc. 3rd Intl Symp. on Integrity of Offshore Structures (IOS'87), Glasgow Univ., pp. 441-463, Sep. 1987.

[3] Laheld, P., "Statistics on Collision Accidents involving Offshore Structures", Introductory Report of IABSE Colloquium on Ship Collision with Bridges and Offshore Structures (IABSE Report Vol. 41), pp. 27-45, Copenhagen, 1983.

[4] Arochiasamy, M., Swamidas, A.S.J. and El-Tahan, H., "Response of Offshore Structures to Bergy-Bit and Iceberg Impacts", in Behavior of Offshoe Structure (Proc. BOSS '85) Ed. Battjes, J.A., Elsevier Science Publishers, Amsterdam, pp. 951-961, 1985.

[5] Choi, K.S., Park, H.I. and Lee, S.G., "A Study on the Structural Design and Construction of Artic Offshore Structures for the Natural Gas Development Project Offshore Sakhalin Island", Korea Science and Engineering Foundation Report, KOSEF 931-1200-012-2, Korea, 1995.

[6] Choi, K.S., "A Damage Mechanics Approach to the Three Dimensional Constitutive Modelling of Ice Deformation", Ph.D. Thesis submitted to M.I.T., 1989.

[7] Watt, B.J., "Design of Prefabricated Offshore Structures for Ice Forces", A State of the Practice Report prepared by the Technical Council on Cold Regions

Engineering of the ASCE, Ed. by S.R. Caldwell and R.D. Crissman, pp. 17-37, 1983.

[8] DYNA3D user's manual, Lawrence Livermore National Laboratory, Rev. 5, 1993.

[9] Cho, S.R., "Design Approximations for Offshore Tubulars against Collisions", Ph.D. thesis submitted to Glasgow University, 1987.

[10] Cowper, G.R. and Symonds, P.S., "Strain-Hardening and Strain-Rate Effects in the Impact Loading of Cantilever Beams", Tech. Report No. 28, Brown University, Rhode Island, 1957.

[11] Ralston, T.D., "An Analysis of Ice Sheet Indentation", Proceedings of the IAHR Symposium on Ice Problems, Lulea,Sweden, Vol. 1, pp. 13-32, 1979.

[12] Mellor, M. and Cole, D.M., "Deformation and Failure of Ice under Constant Stress or Constant Strain-Rate", Cold Regions Science and Technolegy, Vol. 5, pp. 201-219, 1982.